Particle motions in sheared suspensions

XIII. The spin and rotation of disks

By H. L. GOLDSMITH AND S. G. MASON

Physical Chemistry Division, Pulp and Paper Research Institute of Canada, Department of Chemistry, McGill University, Montreal

(Received 15 June 1961)

The motions of single disks suspended in a liquid undergoing Couette flow have been studied in detail. The angular rotation and the axial spin of the disks were found to be in good agreement with the theory of Jeffery, provided the equivalent axis ratio r_e was used instead of the measured axis ratio r. It was found that non-interacting disks move in constant orbits without a tendency to drift into orbits corresponding to a minimum dissipation of energy. Discontinuous changes in orbit were observed to occur following two-body collisions.

1. Introduction

Previous papers in this series have dealt with the rotation (Trevelyan & Mason 1951; Mason & Manley 1956; Bartok & Mason 1957) and spin (Forgacs & Mason 1959) of single rigid rods and spheres in Couette flow. This communication describes the corresponding phenomena for rigid disks. The work became possible following the discovery of a simple method of making suitable particles, and was of interest in order to complete the experimental study of Jeffery's theory (1922) for ellipsoids of revolution.

The only pertinent investigations appear to be those on blood flow through tubes, among them those of Muller (1936, 1939, 1941) who studied the behaviour of large (1300μ diameter) rubber disks, serving as models of human red blood cells undergoing laminar flow through circular tubes; he reported what is interpreted by the present authors to be spin and rotation but did not attempt to analyse the orbits.

Jeffery has given a rigorous theoretical treatment of the rotary motion and axial spin of a single rigid spheroid with centre at the origin of an infinite field of Couette flow defined by

$$u = Gy, \quad v = w = 0,$$

where u, v and w are the respective components of fluid velocity along the X, Y and Z axes and G is the rate of shear. It is assumed that the particle is non-sedimenting, that inertial effects are absent and that there is no slip at the particle-liquid interface.

1.1. *Rotations*

The equations for the angular velocities of the axis of rotation of a spheroid in terms of the spherical polar co-ordinates θ and ϕ with the Z-axis as the polar axis (figure 1) are

$$\frac{d\phi}{dt} = \frac{G}{(r_e^2+1)}[r_e^2\cos^2\phi + \sin^2\phi], \tag{1}$$

$$\frac{d\theta}{dt} = \frac{G(r_e^2-1)}{4(r_e^2+1)}\sin 2\theta \sin 2\theta. \tag{2}$$

These may be integrated to give

$$\tan\phi = r_e \tan(2\pi t/T), \tag{3}$$

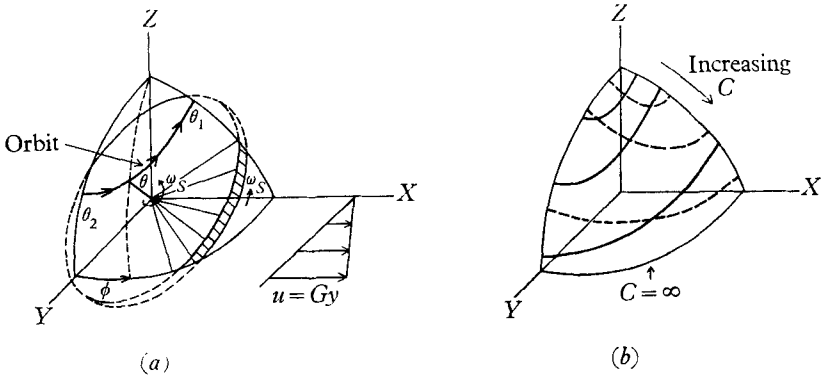

FIGURE 1. Spherical polar co-ordinate system: (*a*) The spherical elliptical orbit of a rotating disk; the co-ordinate system is shown in relation to the shear field. (*b*) A series of orbits for a disk ($r_e < 1$, solid lines) and for a rod ($r_e > 1$, broken lines).

where r_e is the axis ratio a/b, a is the length of the axis of revolution and b the equatorial axis, and T is the period of rotation about the Z-axis given by

$$T = \frac{2\pi}{G}\left(r_e + \frac{1}{r_e}\right). \tag{4}$$

The orbit of the ends of the axis of revolution is the spherical ellipse

$$\tan\theta = \frac{Cr_e}{(r_e^2\cos^2\phi + \sin^2\phi)^{\frac{1}{2}}}, \tag{5}$$

having the following axes:

$$\text{at} \quad \phi = \tfrac{1}{2}\pi, \quad \tan\theta_1 = Cr_e, \tag{6A}$$

$$\text{at} \quad \phi = 0, \quad \tan\theta_2 = C, \tag{6B}$$

where C is the orbit constant. When $r_e > 1$ (prolate spheroid) θ_1 is the major axis of the spherical elliptical orbit, and when $r_e < 1$ (oblate spheroid) the minor axis (figure 1). It follows from (1) that the angular velocity ($d\phi/dt$) of the axes of rotation of two spheroids of $r_e = \sigma$ and $1/\sigma$ are identical when their ϕ's are $\frac{1}{2}\pi$ apart; the periods of rotation T, given by (4), are identical.

When the particles are observed about the Z-axis the projected length $a'(\phi)$ of the axis of revolution in the (X, Y)-plane becomes

$$a'(\phi) = a \sin\theta. \tag{7}$$

The projection of the equatorial plane is an ellipse of axis ratio $s(\phi) \leqslant 1$, where

$$s(\phi) = \frac{b'(\phi)}{b} = \cos\theta, \tag{8}$$

and b' is the projected length of the equatorial diameter at ϕ.

1.2. *Axial spin*

Jeffery predicted that the spheroid undergoes spin about its axis of revolution at an angular velocity ω_s, given by

$$\omega_s = \frac{d\Omega}{dt} = \frac{G}{2}\cos\theta, \tag{9}$$

where Ω is the angle of spin. Equation (9) may be tested by calculating the number of complete axial spins (n) executed in the course of a complete rotation of an oblate spheroid through $\phi = 2\pi$ as was previously done for prolate spheroids (Forgacs & Mason 1959). By elimination of ϕ from (3) and (5),

$$\cos\theta = \frac{A_1}{B_1}\left[\frac{1+\tan^2(2\pi t/T)}{1+\Gamma^2\tan^2(2\pi t/T)}\right]^{\frac{1}{2}} = F(t), \tag{10}$$

where $$A_1^2 = \frac{r_e^2}{1-r_e^2}, \quad B_1^2 = \frac{r_e^2(C^2+1)}{(1-r_e^2)}, \quad \Gamma^2 = \frac{C^2r_e^2+1}{C^2+1}.$$

Thus n becomes

$$n = \frac{\Delta\Omega}{2\pi} = \frac{G}{\pi}\int_0^{\frac{1}{4}T} F(t)\,dt.$$

By substituting $\psi = 2\pi t/T$ and $(1-\Gamma^2) = k_1^2$ in the last equation one finally obtains

$$n = \left(\frac{TG}{2\pi^2}\right)\left(\frac{A_1}{B_1}\right)f(k_1), \tag{11A}$$

where

$$f(k_1) = \int_0^{\frac{1}{2}\pi} \frac{d\psi}{(1-k_1^2\sin^2\psi)^{\frac{1}{2}}}. \tag{11B}$$

Values of the elliptic integral $f(k_1)$ can be obtained from tables, and n calculated for a given r_e and C. Equation (11) is somewhat simpler than the corresponding equation for $r_e > 1$ from which n was evaluated by graphical integration (Forgacs & Mason 1959).

The spin and rotation of rigid rods has previously been shown to follow (1), (2) and (9) provided the equivalent ellipsoidal axis ratio r_e, calculated from the measured period of rotation T and (4), is used instead of the true axis ratio r (Trevelyan & Mason 1951; Mason & Manley 1956; Bartok & Mason 1957; Forgacs & Mason 1959). The same procedure will be followed here in representing disks of thickness a and diameter b as oblate spheroids.

1.3. *Constancy of orbit of single particles*

The question of whether non-interacting ellipsoids take up certain preferred orbits has been under discussion since Jeffery's theory was first published (Taylor 1923; Eirich, Margaretha & Bunzl 1936; Binder 1939). Jeffery postulated that in the steady state the particle will assume an orbit leading to a minimum dissipation of energy, i.e. (i) $C = 0$ for a rod and (ii) $C = \infty$ for a disk, corresponding respectively to (i) steady spin of the axis of revolution parallel to the Z-axis, and (ii) rotation, without spin, of the axis of revolution in the (X, Y)-plane. Mason & Manley (1956) found that the orbital constants of rods showed small random drifts, but concluded that these were due to convection currents generated in the suspending liquid.

Saffman (1956), in a discussion of possible reasons for orbital drift, concluded that inertial effects, neglected in Jeffery's theory, could not account for the observations reported, but that non-Newtonian viscosity of the suspending medium could account for a drift of orbits of rods to $C = 0$.

With the improved experimental technique available it was possible to conduct tests on the constancy of orbit of single disks suspended in a Newtonian liquid in a manner which eliminated important side effects such as convection currents and sedimentation. It was also possible to test (1), (2) and (11).

2. Experimental part

The particles were observed through a microscope directed along the Z-axis of a field of Couette flow in a coaxial cylinder apparatus, with counter-rotating cylinders, which has been described elsewhere (Bartok & Mason 1957; Rumscheidt & Mason 1961).

The disks were made from polystyrene spheres (250–500 μ diameter) by compression between heated platens of a hydraulic press. The thickness of the disks produced was controlled by inserting a layer of brass shim stock between the platens, and the diameter by using different sieved fractions of the polystyrene spheres. The spheres were sprinkled onto the lower platen of the press, taking care as far as was possible to separate each particle; and the temperature was raised to 190 °C, about 100 °C above the softening point, before applying 5000 lb./in^2 pressure. This pressure was maintained until the platens had cooled to room temperature. The disks thus formed were for the most part very uniform; the diameter varied from 400 to 850 μ and the axis ratio r (thickness/diameter) from 0·05 to 0·25. The spheres contained occluded air which lowered their density to 1·05 g/c.c.

The disks were suspended in 50 poise silicone oil (Dow Corning 200 series, $\rho = 0{\cdot}975$ g/c.c.) floated on low viscosity aqueous glycerol to avoid end effects in the Couette apparatus (Bartok & Mason 1957) and the particles were observed in the $y = 0$ layer. Relatively high rates of shear (0·5–2·5 sec^{-1}) were used, enabling the experiments to be performed before appreciable sedimentation occurred. The concentration of the suspensions was negligible; about 25 disks were introduced into 1 l. of oil in each experiment.

The rotational orbits were recorded by taking a cine film through the microscope with vertical illumination from below. A Paillard Bolex 16 mm cine-camera

was used at 15 frames per second, the film subsequently projected on to a horizontal screen and analysed, frame by frame. By means of an electronic timer which actuated a break in the circuit of the microscope lamp, the film was marked at known intervals of time by dark frames, thus providing a time scale. From the elliptical projection of the upper face of a disk, the azimuthal angle ϕ of the axis of rotation of the particle at any given time was obtained from the angle between the major axis of the ellipse b and the X-grid line of the microscope ocular (figure 1). The angle θ was calculated from the axis ratio $s(\phi)$ of the projected ellipse using (8). The axis ratio r was obtained from the measured b, and a, calculated from the measured a' by means of (7).

The number of axial spins (n) per rotation about the Z-axis was measured by following a point on the periphery of the disk and observing the number of complete spins occurring in about 20 rotations.

The constancy of orbit of a given disk was measured by photographing the particle projection in the (X, Y)-plane at $\phi = 0$, corresponding to minimum s, at intervals during 120 particle rotations. A 35 mm automatic camera and beam splitter mounted on the microscope were used for these experiments.

The experiments were made in a thermostatically controlled room at $20\,^{\circ}\mathrm{C} \pm 0{\cdot}5^{\circ}$.

3. Results and discussion

3.1. *General observations*

The rotation and spin of disks, illustrated for a half rotation by the photomicrographs in figure 2, plate 1, were observed visually to be in qualitative agreement with Jeffery's theory. Thus it was found that the angular velocity ($d\phi/dt$) was least when the projected diameter was aligned in the direction of flow and greatest when at right angles, corresponding to $\phi = 0^{\circ}$ and 90° respectively; this is the converse of the case with rods predicted by (1). As the disk rotated, the projected axis ratio $s(\phi)$ went from a maximum at $\theta_1(\phi = \frac{1}{2}\pi)$ to a minimum at $\theta_2(\phi = 0)$ as required by (6) for $r_e < 1$, also the converse of the behaviour of a rod which, for comparison, is illustrated in figure 3 (plate 1). Clearly, without the aid of the theory, it would have been difficult to give a rational description of the orbits of disks, which may explain Muller's failure to do so.

3.2. *Periods of rotation*

In all cases the period of rotation of disks was less than the value predicted by (4) for oblate spheroids using the measured r as previously found with rods (Trevelyan & Mason 1951; Mason & Manley 1956). Thus for the disks the equivalent ellipsoidal axis ratio $r_e > r$, whereas for rods, $r_e < r$.

As with rods r_e/r showed a significant increase with decreasing r (table 1). A plot of r_e/r against log r (figure 4) demonstrates that a smooth curve may be drawn between the points obtained from previous data for rigid rods and those from the present experiments. Additional points obtained from the study of the rotation of disks and rods in a suspension flowing through a tube (Goldsmith & Mason 1961) are also given.

It is evident from table 1 that disks of nearly the same r had nearly equal values of $TG/2\pi$ for quite different orbit constants C, as expected from (1) and (4).

r measured	$\frac{TG}{2\pi}$ measured	r_e Equation (4)	$\frac{r_e}{r}$	c†
0·25	2·96	0·389	1·6	2·82
0·22	2·95	0·382	1·7	4·08
0·22	3·16	0·356	1·6	4·28
0·18	3·37	0·329	1·8	1·70
0·18	3·67	0·296	1·6	∞
0·18	3·76	0·287	1·6	4·31
0·17	3·29	0·339	2·0	3·43
0·10	4·62	0·228	2·3	3·25

† Calculated from measured $s(0)$ or $s(\frac{1}{2}\pi)$ using (6) and (8).

TABLE 1. Measured and equivalent axis ratios of rotating disks.

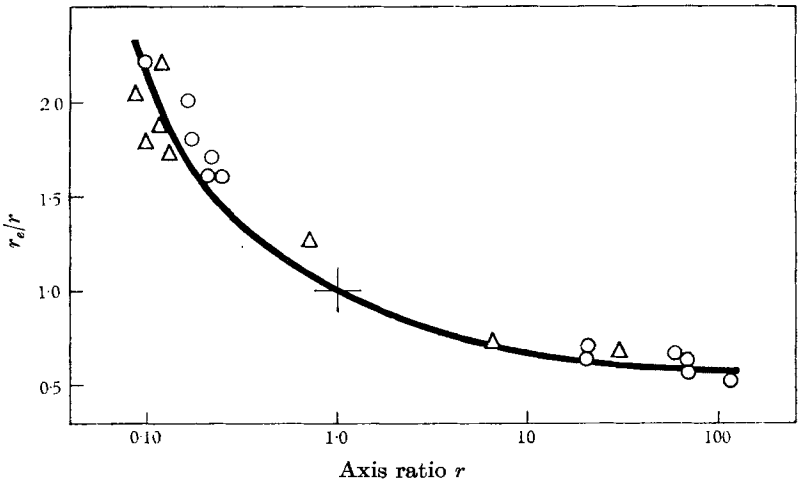

FIGURE 4. The ratio r_e/r as a function of r for rods ($r_e > 1$) and disks ($r_e < 1$). The circles represent experimental points obtained in Couette flow, the triangles those in Poiseuille flow (Goldsmith & Mason 1961). The curve has been drawn through the point shown as a cross, representing the rotation of a sphere (Manley & Mason 1952).

3.3. *Variation of* ϕ

The variation of the azimuthal angle ϕ with time is illustrated in figure 5. It can be seen that the data follow (3) when r_e is used and that $(d\phi/dt)$ is a maximum at $\phi = \pm\frac{1}{2}\pi$ and a minimum when $\phi = 0$. A more sensitive test of the theory is to plot tan ϕ against tan $2\pi t/T$ as shown in figure 6, where it can be seen that the agreement with (3) is excellent, the value of r_e calculated from the slope being the same as that from the measured period of rotation.

3.4. *Variation of θ*

The variation of the angle θ during an orbit is shown in figure 7 where tan θ has been plotted against ϕ for a disk of $r_e = 0{\cdot}146$; agreement with (5) again confirms the theory. The theoretical curve for a rod of $r_e = 1/0{\cdot}146$ having the same orbit constant is shown for comparison.

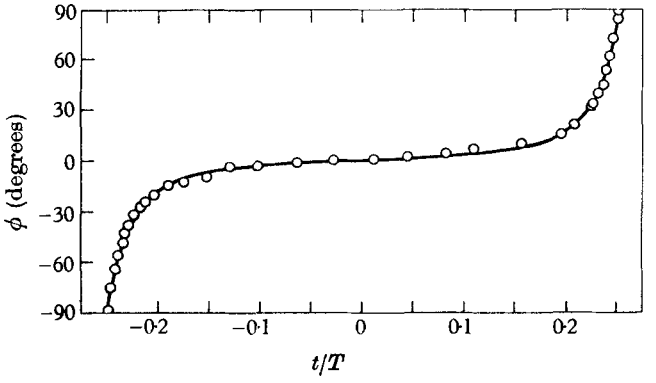

FIGURE 5. Variation of ϕ with time for a rigid disk at $G = 0{\cdot}63$ sec^{-1}. The curve is calculated from (3) using $r_e = 0{\cdot}108$ determined from (4).

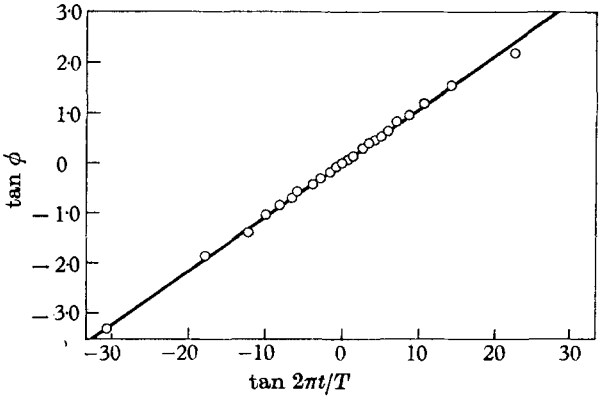

FIGURE 6. Tan ϕ *vs.* tan $2\pi t/T$ for the same particle as in figure 5. The straight line is given by (3) using $r_e = 0{\cdot}108$.

3.5. *Axial spin*

Measured values of n for various values of r_e and C are given in table 2 and are compared with values calculated from (11). In view of the possible error in the orbit constants C due to uncertainties in the measurement of $s(0)$ or $s(\frac{1}{2}\pi)$, the agreement with theory is considered excellent and compares favourably with that found for the spin of rigid rods (Forgacs & Mason 1959).

3.6. *Constancy of orbit*

Orbit constants measured for 5 disks over 120 rotations each are given in table 3. As can be seen the value of the orbit constant showed only random fluctuations except in the first case where it increased by a small amount. Additional evidence

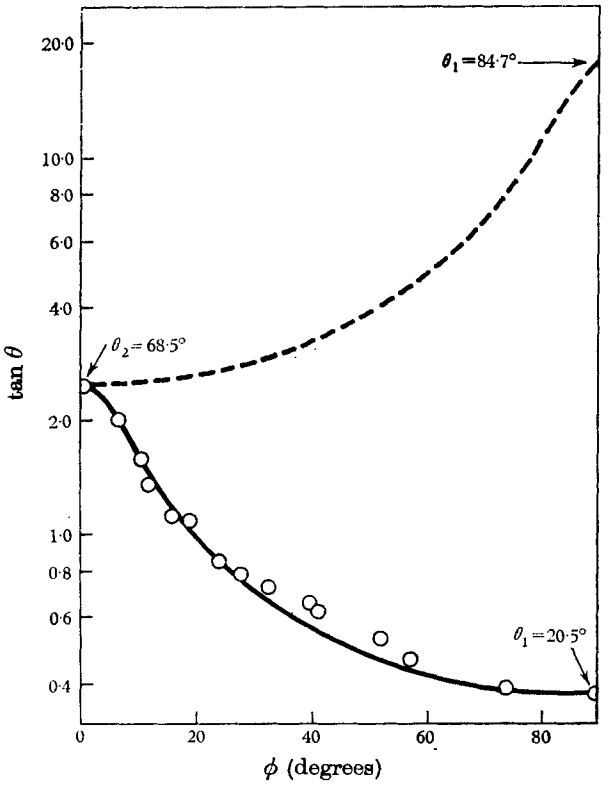

FIGURE 7. Tan θ *vs.* ϕ for a rigid disk with $r_e = 0{\cdot}146$, $C = 2{\cdot}56$, and $G = 0{\cdot}59\ \text{sec}^{-1}$. Points are experimental values and the solid curve is calculated from (5). The dotted curve is calculated for a rigid rod of $r_e = 1/0{\cdot}146$ and $C = 2{\cdot}56$.

Mean T sec	G sec^{-1}	r_e Equation (4)	θ_2 degrees	C	$f(k_1)$	Calculated n Equation (11)	Observed n spins/rev.	$\frac{n_{obs.}}{n_{calc.}}$
8·9	2·26	0·382	76·0	4·08	2·26	0·12	0·11	0·92
8·5	2·38	0·364	77·0	4·28	2·32	0·11	0·13	1·18
10·2	2·32	0·287	77·0	4·31	2·45	0·15	0·20	1·33
7·6	2·43	0·389	70·3	2·82	2·16	0·23	0·18	0·78
93·6	0·63	0·107	86·0	14·2	3·75	0·54	0·53	0·98
								Mean = 1·0

TABLE 2. Axial spin of disks.

Mean T sec	G sec^{-1}	r_e	C after N rotations				
			$N = 0$	$N = 30$	$N = 60$	$N = 90$	$N = 120$
6·0	2·87	0·433	1·60	1·83	1·83	1·93	1·93
11·4	1·82	0·339	3·44	3·44	3·51	3·43	3·43
11·3	2·04	0·296	∞	∞	∞	∞	∞
12·5	2·33	0·228	3·25	3·25	3·26	3·27	3·24
14·3	1·48	0·329	1·67	1·72	1·73	1·67	1·61

TABLE 3. Constancy of disk orbits.

in support of the constancy of the orbits was obtained from the axial spin measurements where again there were only slight fluctuations in C over 75 to 100 rotations.

It was observed for one disk where the measurements were carried out over a much longer period of time that as the disk sedimented appreciably the orbit constant progressively decreased.

3.7. *Interactions*

The concentration of the suspensions of the disks were so low that interactions between particles were very rare. However for the few 2-body collisions observed it was evident that after the particles separated each rotated in a different orbit. This discontinuous change in C of each particle on collision is similar to that previously observed with rods (Mason & Manley 1956).

4. Conclusions

It is evident that, as with rods, Jeffery's theory of spin and rotation holds for disks provided r_e is used in place of r to allow for the difference in shape from a spheroid. It is concluded, moreover, that non-interacting particles move in constant orbits and that the Jeffery minimum viscosity hypothesis is invalid. The behaviour of disks in Poiseuille flow through a circular tube where G is variable is considered in a forthcoming paper by the present authors.

This work was supported by the Defence Research Board of Canada DRB Grant 9510-05.

REFERENCES

BARTOK, W. & MASON, S. G. 1957 *J. Colloid Sci.* **12**, 243.

BINDER, A. 1939 *J. Appl. Phys.* **10**, 711.

EIRICH, F., MARGARETHA, H. & BUNZL, M. 1936 *Kolloid Z.* **75**, 20.

FORGACS, O. L. & MASON, S. G. 1959 *J. Colloid Sci.* **14**, 457.

GOLDSMITH, H. L. & MASON, S. G. 1961 *J. Colloid Sci.* (in the Press).

JEFFERY, G. B. 1922 *Proc. Roy. Soc.* A, **102**, 161.

MANLEY, R. St. J. & MASON, S. G. 1952 *J. Colloid Sci.* **7**, 354.

MASON, S. G. & MANLEY, R. St. J. 1956 *Proc. Roy. Soc.* A, **238**, 117.

MULLER, A. 1936 *Abhandlungen Zur Mechanik der Flüssigkeiten.* Freiburg, Switzerland: University of Freiburg Press.

MULLER, A. 1939 *Archiv. Kreislauf.* **4**, 105.

MULLER, A. 1941 *Archiv. Kreislauf.* **8**, 245.

RUMSCHEIDT, F. D. & MASON, S. G. 1961 *J. Colloid. Sci.* **16**, 210.

SAFFMAN, P. G. 1956 *J. Fluid Mech.* **1**, 540.

TAYLOR, G. I. 1923 *Proc. Roy. Soc.* A, **103**, 58.

TREVELYAN, B. J. & MASON, S. G. 1951 *J. Colloid. Sci.* **6**, 354.

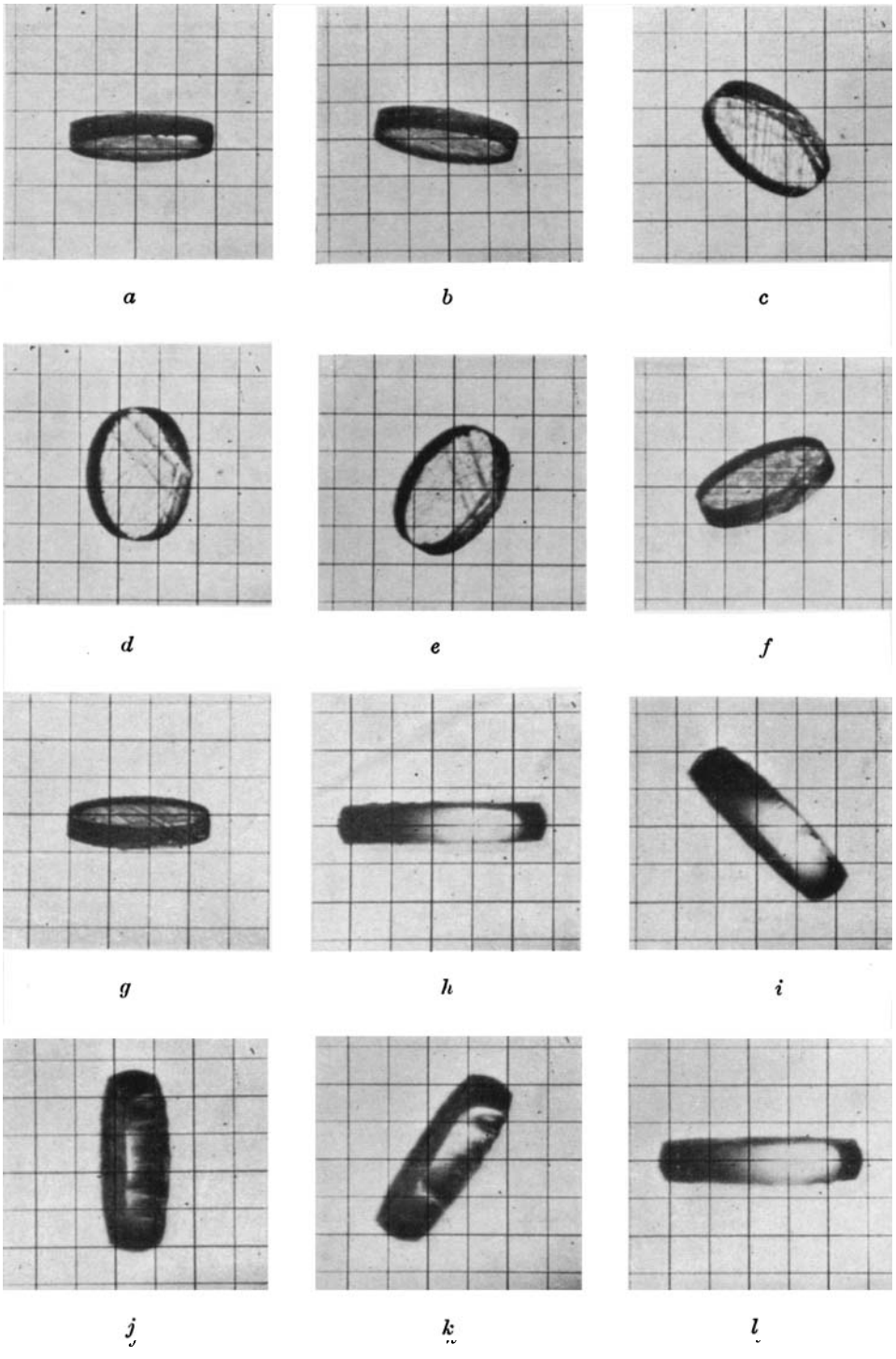

FIGURE 2, PLATE 1. Photomicrographs of half rotation of polystyrene disks viewed along the Z-axis of a field of Couette flow. (a) to (g) : particle of axis ratio $r = 0{\cdot}19$, $C = 4{\cdot}04$. Magnification: distance between grid lines = 193μ, $\phi = 0°$, $11°$, $42°$, $90°$, $-61°$, $-46°$, and $0°$ respectively. (h) to (l): particle of axis ratio $r = 0{\cdot}20$, $C = \infty$. Magnification: distance between grid lines = 111μ, $\phi = 0°$, $42°$, $90°$, $-55°$ and $0°$ respectively.

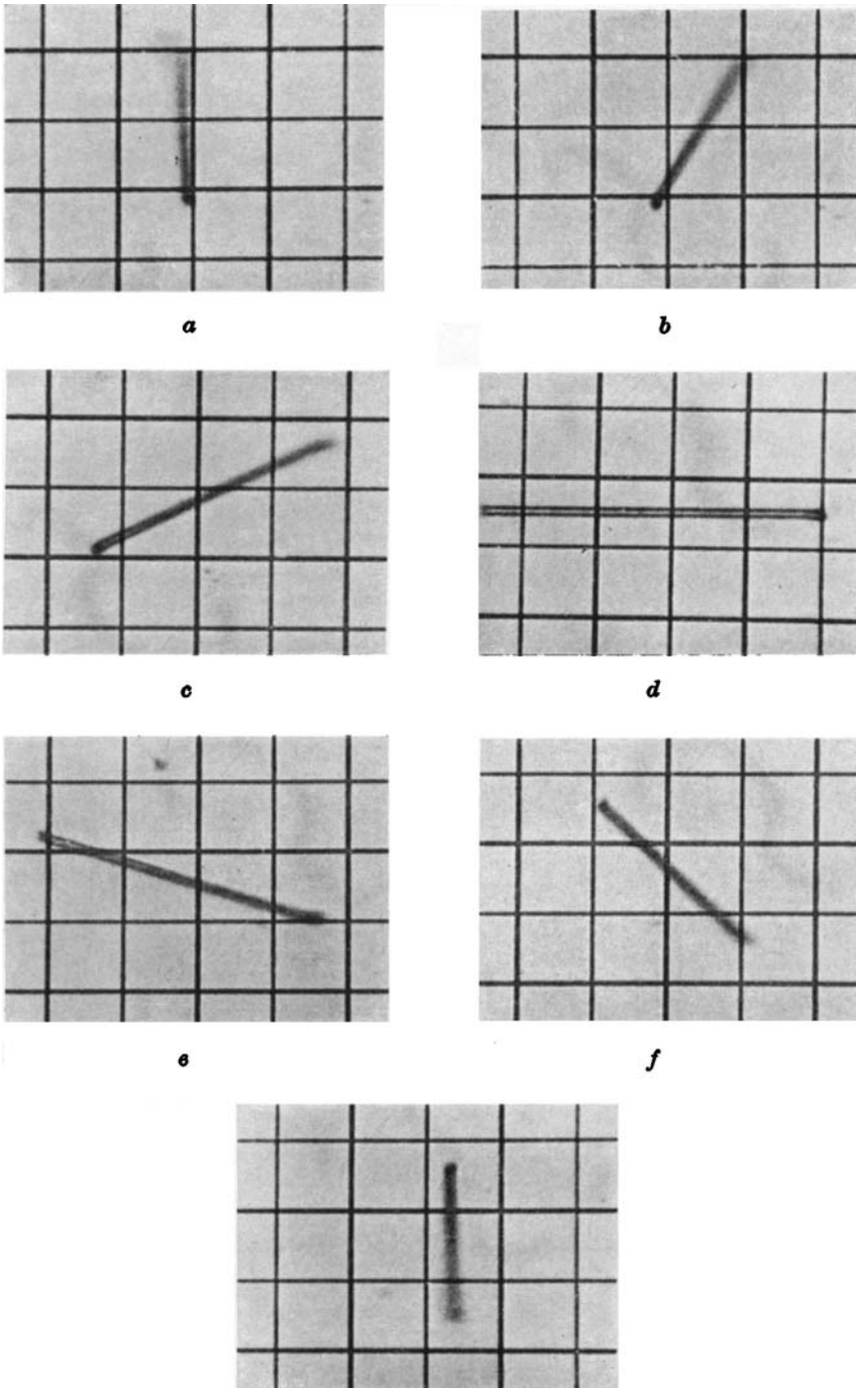

FIGURE 3, PLATE 1. Photomicrographs of the half rotation of a dacron rod viewed along the Z-axis of a field of Couette flow. Particle axis ratio $r = 29$, $C = 0{\cdot}52$. Magnification: distance between grid lines $= 81\mu$. From (a) to (g): $\phi = -1°, 30°, 62°, 90°, -73°, -47°$ and $0°$ respectively.